https://doi.org/10.1038/s44298-025-00111-2

A decade of grapevine red blotch disease epidemiology reveals zonal roguing as novel disease management

M. T. Flasco[1,3] ✉, D. W. Heck[1,4], E. J. Cieniewicz[1,5], M. L. Cooper[2], S. J. Pethybridge[1] & M. F. Fuchs[1]

Red blotch disease, a threat to the grape industry, is caused by grapevine red blotch virus. This work is the first to study epidemiological patterns in a vineyard over the course of a decade, revealing an increase in disease incidence from 3.9% in 2014 to 36.4% in 2023 with rapid virus spread proximal to a transmission hotspot. Logistic and exponential models provided the best fit of spread in areas of high and low disease incidence and aggregation, respectively. An inverse spatial incidence of virus strains 1 and 2 suggested secondary spread mostly from diseased to neighboring vines and virus influx from background sources. Precipitation (3-4 years later) and air temperature (the same or 1 year later) significantly influenced epidemic parameters. Finally, asymptomatic infections contributed to spatial aggregations at increasing lags. These findings were salient for considering zonal roguing, the removal of diseased and surrounding vines, as a disease management option.

Plant viral disease epidemiology is influenced by the host, characteristics of the virus, vector dynamics, spatiotemporal distribution of infected individuals in a population, and ecological factors that collectively affect virus transmission[1,2]. Knowledge of disease epidemiology at individual and landscape scales is foundational for the development of evidence-based guidelines to reduce disease incidence, limit virus spread and mitigate crop loss.

Red blotch disease was first identified in 2008[3] and has since emerged as a serious threat to grape production in North America[4–7]. The disease has also been reported in Switzerland, South Korea, Mexico, Argentina, India, Italy, France, Australia, and Iran[8]. Red blotch disease is caused by grapevine red blotch virus (GRBV, species *Grablovirus vitis*, genus *Grablovirus*, family *Geminiviridae*)[9]. Isolates of GRBV belong to two distinct phylogenetic clades that have up to 91.5% sequence identity[5], and both are involved in disease etiology[9]. For simplicity, herein GRBV isolates of phylogenetic clades 1 and 2 will be referred to as strains 1 and 2.

The natural host range of GRBV is limited to *Vitis* species, including grape cultivars[10–13], rootstocks[9,14], and free-living grapevines in northern California[14–17] and southern Oregon[18]. The global distribution of GRBV has been attributed to the dissemination of infected planting material, distribution of infected cuttings and budwood, and graft transmissibility of the virus[4,7,19]. Diseased, red-berried wine grape cultivars display characteristic foliar reddening, poor fruit yield and quality, and off-balance wines with atypical aromas and flavors[4,6,7,20,21]. Economic losses of red blotch disease range from $2200 to $68,548 per hectare over a vineyard's productive lifespan[22].

Secondary spread of red blotch disease has been described in northern California[14,17,23–25] and southern Oregon[18,26]. In vineyards of northern California, secondary spread has been attributed to *Spissistilus festinus* (Say) (Hemiptera: Membracidae), the three-cornered alfalfa hopper, which transmits the two GRBV strains in a circulative and non-propagative manner[27,28]. Acquisition of the virus by *S. festinus* in northern California vineyards occurs mostly in early summer (June and July)[28] when vector populations peak[24,29–32], infections are asymptomatic, and GRBV titer is lower compared to later in the growing season[33–35]. The spatiotemporal distribution of red blotch diseased vines has been characterized, but such studies have not exceeded four years[14,18,23,24,26], a relatively short period for a disease epidemic in a perennial fruit crop such as grapevine for which the productive lifespan of a vineyard is at least 25 years.

The aim of our study was to characterize the spatiotemporal spread of GRBV over a decade in a red blotch-affected 'Cabernet franc' vineyard in California and identify unique disease epidemiological attributes using descriptive and quantitative statistics. We hypothesized that disease spread is driven by local transmission in relation to incidence and aggregation. We also hypothesized that different disease progression models would fit the observed spread dynamics within the study vineyard and that environmental factors would influence spread parameters. Results were used to make inferences on potential sources of virus inoculum, assess the spatial

[1]Plant Pathology and Plant-Microbe Biology Section, Cornell University, Geneva, NY, USA. [2]UC Cooperative Extension, University of California, Napa, CA, USA. [3]Present address: Plant Pathology and Crop Physiology, Louisiana State University Agricultural Center, Baton Rouge, LA, USA. [4]Present address: Plant Pathology and Plant-Microbe Biology, Cornell University, Long Island Horticultural Research and Extension Center, Riverhead, NY, USA. [5]Present address: Plant and Environmental Sciences, Clemson University, Clemson, SC, USA. ✉e-mail: mflasco@agcenter.lsu.edu

relationship between infected and surrounding vines, and evaluate the associations between environmental factors and disease dynamics. Our findings were transformative for refining red blotch disease management recommendations in vineyards experiencing secondary spread.

Results

Distinct rates of red blotch disease progress identified across the vineyard

Red blotch disease incidence was mapped in a 2-hectare 'Cabernet franc' vineyard affected by red blotch disease by visually inspecting individual vines ($n = 7729$) in early to mid-October for a decade. Disease incidence increased significantly ($p < 0.001$; Supplemental Table 1) from 3.9% in 2014 to 36.4% in 2023 across the entire vineyard (Fig. 1A, Supplemental Table 2). The exponential model provided the best fit disease epidemic ($p < 0.001$; Supplemental Table 1) with an estimated rate of disease progress (r), a unitless model parameter from non-linear regression analysis, of 0.227 ($p < 0.001$; Fig. 1A). The logistic model, which has equivalent parameters to the exponential model when disease incidence is low, was a better fit to the entire epidemic. It is estimated the epidemic would take ~14.2 years to reach 50% incidence (Supplemental Table 3). Disease spread was more substantial in the eastern area of the vineyard where a disease focus, an area of elevated disease incidence and aggregation of diseased vines, was first detected in 2014. From this area, a gradient of diseased vines was observed westward (Fig. 1A).

Five subsections (A-E) were delineated across the entire vineyard based on distance from the predicted disease focus and disease incidence (Fig. 2A). In all subsections, disease incidence increased since 2014 at different rates (Fig. 2B). While temporal disease analyses best fitted an exponential model of disease spread in the study vineyard and subsections A-C farthest from the disease focus, a logistic model provided the best fit of spread for subsections D and E closest to, and within the disease focus, respectively (Supplemental Table 1 and 4). A higher disease incidence (y) was observed in subsection E than in subsections A-D when considering all assessments ($p < 0.001$; Fig. 2B; Supplemental Table 5). Consequently, in subsection A with the lowest rate of disease progress ($r = 0.140$; Supplemental Table 3), 50% incidence was estimated to occur 23.5 years after the start of the epidemic. In subsection E, closest to the predicted disease focus, with a higher rate of disease progress ($r = 0.698$) and initial incidence ($y_0 = 0.07$), 50% disease incidence was predicted to be reached 3.6 years after the epidemic began, while it was estimated to vary between 8.9 and 16.6 years in subsections B-D (Supplemental Table 3).

Asymptomatic GRBV infections result in underestimations of disease incidence

Testing of vines for the presence of GRBV in subsections A-E revealed asymptomatic infections of both virus strains (Fig. 2B; Table 1). Across the five subsections, the incidence of asymptomatic infections was 9.1% (162/1,783) in 2023, and ranged from 0.8% to 13.8% in the five subsections (Fig. 2B). In subsection B, along the vineyard edge opposite the disease focus, asymptomatic vines were primarily infected with strain 1 (7.7%, 26/336) compared to strain 2 (3.9%, 9/336), while symptomatic vines were infected with strain 1 (4.8%, 16/336) or strain 2 (6.5%, 22/336) at an approximately equal ratio.

Opposing spatial prevalence of GRBV strains 1 and 2 occur in diseased vines throughout the vineyard

Across the five subsections, strain 2 was prevalent in infected vines (26.1%, 465/1783) compared to strain 1 (13.7%, 240/1783) (Fig. 2B, Table 1). However, significant differences in the incidence of strains 1 and 2 were detected in subsections A and E, but not in subsections B-D (Fig. 2B; Table 1). In addition, the same strain was consistently found in vines that tested positive for GRBV in 2022 and 2023 with no evidence of coinfection by the two strains.

Spatiotemporal disease spread dynamics indicate aggregations of diseased vines

Spatiotemporal analyses revealed aggregations of diseased vines throughout the entire vineyard each year (Fig. 1C, D). The level of aggregation increased over time for both distribution-based statistics (D and θ) and the index of aggregation of Spatial Analysis by Distance IndicEs (SADIE), I_a. D ranged from 1.95 in 2014 to 2.95 in 2022, and the level of aggregation (θ) from 0.412 to 1.82 during the same period at the smallest spatial scale (2 × 2 quadrats). I_a values ranged from 5.18 in 2014 to 10.3 in 2020 at the 2 × 2 quadrat size. The magnitude of aggregation of diseased vines was also affected by the spatial scale. As the quadrat size increased, higher D, and lower θ and I_a values were obtained (Fig. 1B, D), from which we inferred that GRBV spread occurred mostly to neighboring vines ($p < 0.05$; Supplemental Table 6).

Aggregations of diseased vines were similarly observed in four of the five subsections of the vineyard with variable trends based on D (Supplemental Tables 7–11). In subsection E, closest to the initial disease focus (Fig. 2A), the spatial pattern of diseased vines was significantly aggregated in 2017–2023 (Fig. 2C) with θ significantly increasing in 2015 compared to 2014. In subsection A, opposite the initial disease focus, a significant aggregation of diseased vines was only observed in 2022 (Fig. 2C). A random distribution of diseased plants was observed in subsections B and C, except in subsection B in 2022 ($p = 0.03$) (Fig. 2C). In subsection D, close to the initial disease focus (Fig. 2A), disease incidence substantially increased from 4.6% in 2020 to 20.8% in 2021 ($p < 0.001$; Fig. 2C) with the level of aggregation significantly increasing in 2022 and 2023 (Fig. 2).

In subsection E nearest the disease focus, 2 × 2 quadrats were significantly aggregated from 2015 to 2020 (Fig. 2D). In subsection A, furthest from the disease focus, aggregations at the 2 × 2 quadrat were significant in all years (Fig. 2D). In subsection B, similarly away from the disease focus, 2 × 2 quadrats were only significantly aggregated in 2023, and in 2021–2023 in subsection D (Fig. 2D).

To further characterize disease spread, SADIE was applied to vines infected with strains 1 or 2 within each subsection (Fig. 2D). In subsection A, aggregations of 2 × 2 quadrat vines infected with strain 1 were significant in all years, while vines infected with strain 2 were significantly aggregated only in 2014–2017 (Fig. 2D). The converse was true in subsection E, where vines infected with strain 1 were first detected in 2015 and the distribution was random in each year (Fig. 2D), but vines infected with strain 2 were predominant (80.4%, 193/240) and spatially aggregated each year from 2016–2020 (Fig. 2D). In subsection D, vines infected with strain 1 were aggregated in 2021 and 2022; and vines containing strain 2 were aggregated from 2020–2023 (Fig. 2D). In subsections B and C, opposite the disease focus, the distribution of strains 1 and 2 was random in all years, except for strain 2 in subsection C in 2023 (Fig. 2D, Supplemental Tables 7–11). These data highlight non-uniform aggregated spread from neighboring vines.

Spatial relationships between GRBV-infected and surrounding vines varies within the vineyard

Varying spatial relationships between a diseased vine and its surrounding vines were observed in each vineyard subsection by join-count analysis (Supplemental Table 12). In subsection A, farthest from the disease focus, significant aggregation was limited to one neighboring vine (one spatial lag) in either direction (Fig. 3). In subsections B and C, where a random distribution was depicted by SADIE (Fig. 2D), aggregation was significant again at one spatial lag within and between rows (Fig. 3). In subsection B, diseased plants at one spatial lag in the rook position were also aggregated (Fig. 3). These data indicated a single diseased vine may increase the likelihood of a neighboring vine within row, across row and diagonal also being symptomatic.

By considering asymptomatic and symptomatic infections, there was often a greater lag of significant spatial aggregation (Supplemental Table 12). In subsection A, spatial aggregation was significant up to two vines within the row of an infected vine for both strains 1 and 2 independently ($z = -2.03$ and $z = -1.96$, respectively; Fig. 3). In subsection B, vines infected with strain 1 were aggregated at two spatial lags within the row ($z = -2.96$), one spatial lag across the row ($z = -2.96$), but not in the rook position; while vines infected with strain 2 were aggregated at two spatial lags within and across rows, and in the rook position (Fig. 3). In subsection C, internal to the vineyard and opposite the disease focus, vines infected with strain 1 were

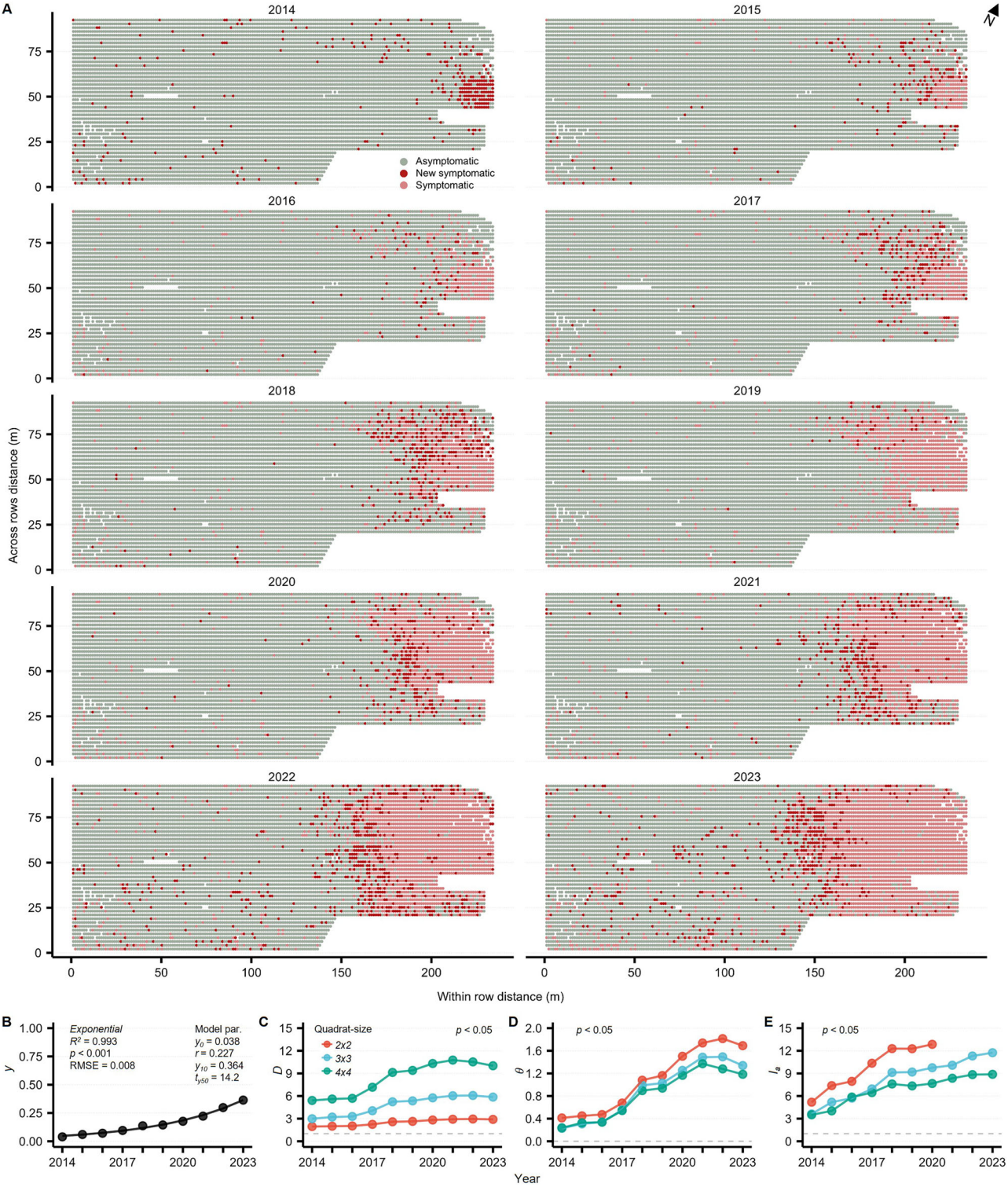

Fig. 1 | Disease incidence and spatial statistics of a 2-hectare red blotch diseased 'Cabernet franc' vineyard in Napa Valley, California. A Schematic images of the diseased vineyard in which vines exhibiting red blotch disease symptoms for the first time are indicated in red, those symptomatic in prior surveys in pink, and asymptomatic vines in green. Missing or dead vines are in white. Each map represents each year of study from 2014–2023. **B** Disease incidence (y) from 2014 to 2023. The x-axis represents years of the study, the y-axis represents the proportion of diseased vines over the total number of vines in the vineyard. Regression statistics values are listed. An exponential model best fit the disease epidemic with supporting statistics listed. **C** Index of dispersion from 2014 to 2023 using 2 × 2, 3 × 3, and 4 × 4 vine quadrats. The x-axis represents years of the study, the y-axis represents the index of dispersion (D) in which $D > 1$ indicates aggregated disease patterns. **D** Beta-binomial distribution fitting calculated using 2 × 2, 3 × 3, and 4 × 4 vine quadrats. The x-axis represents years of the study, the y-axis represents the measure of disease heterogeneity, θ. **E** Spatial Analysis by Distance IndicEs (SADIE) analysis using 2 × 2, 3 × 3, and 4 × 4 vine quadrats. The x-axis represents study year, the y-axis represents the index of aggregation I_a in which $I_a > 1$ indicates an aggregated pattern.

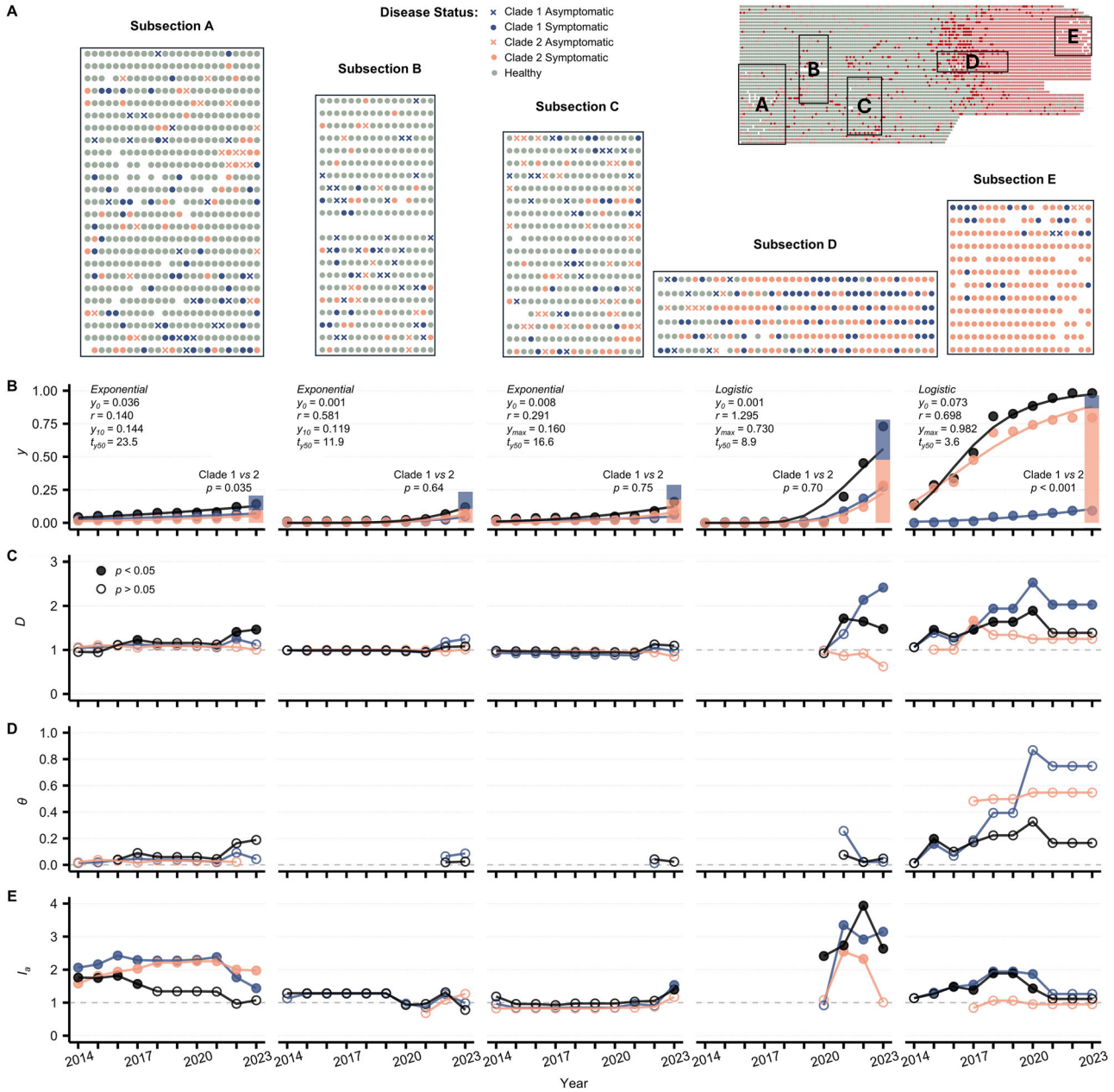

Fig. 2 | Disease incidence, spatiotemporal statistics, and occurrence of asymptomatic infections in five subsections (A-E) of a 2-hectare red blotch diseased 'Cabernet franc' vineyard in Napa Valley, California from 2014 to 2023. A Red blotch disease incidence map of the 'Cabernet franc' study vineyard in 2023 with five subsections in which every vine was tested for grapevine red blotch virus (GRBV) by PCR, and strains 1 and 2 by restriction fragment length polymorphism in 2022 and 2023. For subsections, vines infected with GRBV strain 1 shown in blue and strain 2 in pink. Vines testing positive for GRBV and symptomatic are depicted as a closed circle, those positive for GRBV and asymptomatic are shown as an 'X'. Vines negative for GRBV by PCR and not exhibiting symptoms are shown in green, and open spaces indicate missing or dead vines. **B** Disease incidence by year for each subsection. Circles are observed values, and lines are predicted incidences using best-fitting models. The model of best fit and supporting statistics associated with symptomatic vines is depicted in each panel. Pairwise-t-tests were conducted to determine if the incidence of GRBV strain 1 compared to strain 2 was statistically significant, p values are provided for each subsection. The total number of infected vines represented by bar plots in 2023 includes symptomatic and asymptomatic infections. The y-axis represents the proportion of diseased vines over the total number of vines in the subsection. Non-linear regression and best-fitting model statistics are listed. **C** Index of dispersion (D) calculated each year of the study using 2×2 vine quadrats. $D > 1$ indicates aggregated disease patterns. **D** Aggregation index (θ) of the beta-binomial distribution. $\theta > 0$ indicates an aggregated pattern. **E** Index of aggregation (I_a) of the Spatial Analysis by Distance IndicEs (SADIE) analysis. $I_a > 1$ indicates an aggregated pattern. For panels, **B**–**E**, vines infected with GRBV strain 1 are in blue, strain 2 in pink, and all infected vines in black. Statistical tests with p values less than the level of significance, $\alpha = 0.05$, are represented by a closed circle, those greater than the level of significance are an open circle in **C**, **D**.

aggregated at only one spatial lag across the row while vines infected with strain 2 were aggregated at the same spatial lag but across and within rows (Fig. 3). In subsection D, internal to the vineyard closest to the disease focus, with 30.8% (74/240) and 48.3% (116/240) of the vines infected with strain 1 or 2, respectively, spatial aggregation extended up to three spatial lags within and across rows, and in the rook position (Fig. 3). Within the disease focus, subsection E had 9.2% (22/240) and 80.4% (193/240) of the vines infected with strain 1 or 2, respectively (Table 1) with significant aggregation at one spatial lag within and across rows for strain 1, and at six spatial lags within and across rows, and in the rook position for strain 2 (Fig. 3). These data

Table 1 | Incidence of grapevines infected with strains 1 or 2 of grapevine red blotch virus (GRBV) in five subsections (A–E) of a 2-hectare 'Cabernet franc' vineyard in Napa Valley, California from 2014 to 2023

	A[a]		B		C		D		E	
	Strain 1[b]	Strain 2	Strain 1	Strain 2	Strain 1	Strain 2	Strain 1	Strain 2	Strain 1	Strain 2
2014[c]	16/625[d] (2.6%)	10/625 (1.6%)	1/336 (0.3%)	2/336 (0.6%)	4/342 (1.2%)	4/342 (1.2%)	0/240 (0%)	0/240 (0%)	0/240 (0%)	31/240 (12.9%)
2015	21/625 (3.4%)	11/625 (1.8%)	2/336 (0.6%)	2/336 (0.6%)	6/342 (1.8%)	5/342 (1.5%)	1/240 (0.4%)	0/240 (0%)	1/240 (0.4%)	63/240 (26.3%)
2016	22/625 (3.5%)	12/625 (1.9%)	2/336 (0.6%)	2/336 (0.6.%)	7/342 (2.1%)	5/342 (1.5%)	2/240 (0.8%)	0/240 (0%)	1/240 (0.4%)	74/240 (30.8%)
2017	25/625 (4%)	14/625 (2.2%)	2/336 (0.6%)	2/336 (0.6%)	7/342 (2.1%)	6/342 (1.8%)	2/240 (0.8%)	0/240 (0%)	3/240 (1.3%)	114/240 (47.5%)
2018	28/625 (4.5%)	18/625 (2.9%)	3/336 (0.9%)	2/336 (0.6%)	7/342 (2.1%)	7/342 (2.5%)	2/240 (0.8%)	0/240 (0%)	11/240 (4.6%)	164/240 (68.3%)
2019	28/625 (4.5%)	18/625 (2.9%)	3/336 (0.9%)	2/336 (0.6.%)	7/342 (2.1%)	7/342 (2.5%)	2/240 (0.8%)	0/240 (0%)	13/240 (5.4%)	166/240 (69.2%)
2020	29/625 (4.6%)	18/625 (2.9%)	3/336 (0.9%)	4/336 (1.2%)	9/342 (2.6%)	7/342 (2.5%)	4/240 (1.7%)	0/240 (0%)	14/240 (5.8%)	178/240 (74.2%)
2021	29/625(4.6%)	20/625 (3.2%)	4/336 (1.2%)	5/336 (1.5%)	9/342 (2.6%)	8/342 (2.3%)	21/240 (8.8%)	7/240 (2.9%)	18/240 (7.5%)	187/240 (77.9%)
2022	43/625 (6.9%)	30/625 (4.8%)	8/336 (2.4%)	13/336 (3.9%)	12/342 (3.5%)	18/342 (5.3%)	44/240 (18.3%)	29/240 (12.1%)	22/240 (9.2%)	191/240 (79.6%)
2023	48/625 (7.7%)	39/625 (6.24%)	16/336 (4.8%)	22/336 (6.5%)	21/342 (6.1%)	32/342 (9.4%)	66/240 (27.5%)	68/240 (28.3%)	22/240 (9.2%)	191/240 (79.6%)
Asymptomatic[e]	20/625 (3.2%)	21/625 (3.4%)	26/336 (7.7%)	9/336 (3.9%)	38/342 (5.3%)	29/342 (8.5%)	8/240 (2.9%)	9/240 (4.2%)	0/240 (0%)	2/240 (0.8%)
Total[f]	68/625 (10.9%)	60/625 (9.6%)	42/336 (12.5%)	35/336 (10.4%)	39/342 (11.4%)	61/342 (17.8%)	74/240 (30.8%)	116/240 (48.3%)	22/240 (9.2%)	193/240 (80.4%)
Pairwise *t* test (*p*)[g]	0.030		0.644		0.753		0.696		<0.001	

[a]Subsections of a 'Cabernet franc' vineyard.
[b]GRBV strain (1 or 2) in infected vines.
[c]Year in which visual surveys were conducted.
[d]Proportion of grapevines exhibiting foliar reddening indicative of red blotch disease over the total number of vines in the subsection.
[e]Proportion of vines not exhibiting foliar symptoms but infected with GRBV determined by PCR in 2023.
[f]Proportion of the total number of vines infected with GRBV over the total number of vines in each subsection.
[g]Probability value (*p*) of a pairwise-t-test (Bonferroni) adjustment comparing epidemic of symptomatic vines caused by strains 1 and 2 of GRBV within each vineyard subsection.

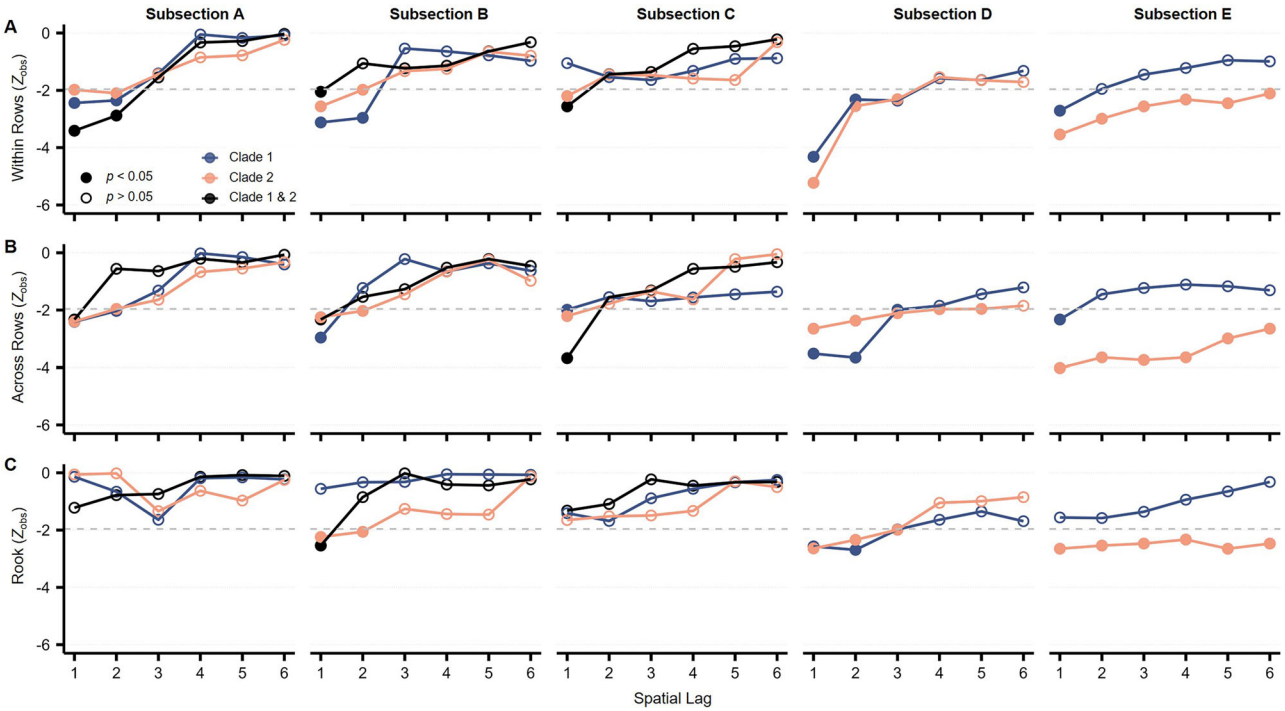

Fig. 3 | Spatial relationship amongst the vines neighboring a single diseased vine across all five subsections of the 2-hectare red blotch diseased 'Cabernet franc' vineyard in Napa Valley, California. Join-count analyses were conducted for all grapevine red blotch virus (GRBV)-infected vines (black), vines infected with a GRBV strain 1 (blue) or strain 2 (pink). Z-statistics less than -1.96 (closed circle) indicate vines surrounding an infected vine at the assigned spatial lag are likely to be infected. A lack of spatial aggregation, Z-statistics greater than -1.96, are represented by open circles. The *x*-axis represents the spatial lag, or the number of neighboring vines surrounding an infected vine, **A** within the same row, **B** across rows, or, **C** in a rook or diagonal pattern. The *y*-axis represents the Z-statistic of the join-count analysis.

indicated the spatial lag surrounding an infected vine is affected by the level of aggregation and the presence of asymptomatic infections.

Precipitation and spring air temperature are negatively associated with epidemic parameters

Correlation analyses indicated an association between weather data, such as air temperature and precipitation, on two epidemic parameters (Fig. 4), though these associations varied based on the time of year (Supplemental Table 13). In spring (March–June), minimum air temperature was negatively associated with disease incidence and rate of spread in the same season ($r = -0.076$ and $r = -0.65$, respectively) or one year later ($r = -0.67$ and $r = -0.66$, respectively). Spring precipitation was also negatively associated with the rate of disease spread and disease incidence three ($r = -0.64$) or four ($r = -0.64$) years later (Fig. 4). In the summer (June-September), precipitation was negatively associated with disease incidence ($r = -0.68$) and rate of spread ($r = -0.71$) three years later (Fig. 4).

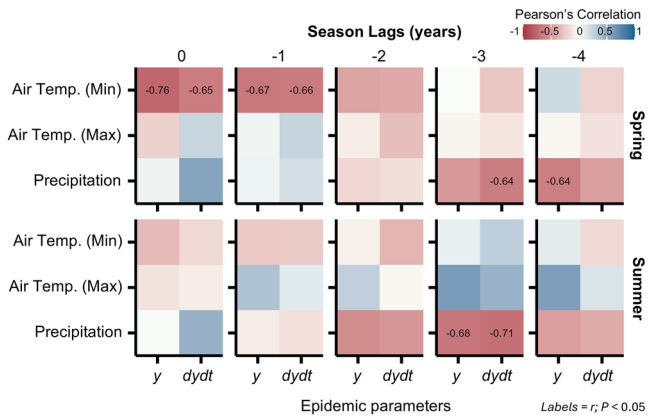

Fig. 4 | Pearson's correlation coefficient depicting the association between weather data and epidemiological metrics with seasonal lag in a diseased 'Cabernet franc' vineyard in Napa Valley, California. Climatic variables shown on the *y*-axis were correlated to disease incidence (*y*) and disease rate (*dy/dt*) found on the *x*-axis for spring (March–June) and summer (June–September). Results were calculated for each year of the study, 2014–2023 wherein associations with epidemic parameters were determined based on weather data of the same year (lag = 0), and seasonal lags one to four years prior to the reported epidemic parameters (lag = −1 and −4, respectively). Seasonal lags of −1, −2, −3, and −4 relied on weather data reported in 2013–2022, 2012–2021, 2011–2020, and 2010–2019, respectively. Red and blue colors represent a negative and positive correlation, respectively, with higher values of *r* represented by darker shades. Correlation coefficient values are presented if significant following the *F* distribution ($p \leq 0.05$).

Discussion

A 3.36% average annual increase in red blotch disease incidence was observed over a 10-year epidemic in a 'Cabernet franc' vineyard in northern California (Fig. 1B). This is consistent with *S. festinus*-mediated transmission rates obtained in the greenhouse (4–42%)[27,36] and in the vineyard under controlled (2–10%)[28] or natural (0.3–28%)[14,18,23,24,26] conditions. Distinct spread dynamics were observed in different areas of the 2-ha vineyard (Fig. 2) with a disease focus at the eastern edge of the vineyard, near subsection E (Fig. 2D). The temporal analyses depicted different models for different epidemic stages (Fig. 2). In subsections A to C, the relatively low initial disease incidence likely led to an unconstrained expansion of infected vines, capturing an early, faster growth phase consistent with exponential spread. In contrast, spread in subsections D and E began with a higher initial incidence, suggesting more established disease foci and larger inoculum sources that would, over time, introduce natural constraints on further expansion. These constraints can occur due to the limited availability of uninfected vines, vector movement restrictions (e.g., shorter distances between infected and healthy vines that reduce the "search space" for vectors), and possible localized resource depletion for vectors. Consequently, the logistic model was more appropriate in subsections D and E (Fig. 2B).

Nevertheless, in subsection A, opposite the disease focus, diseased vines were spatially aggregated, though the final disease incidence was lower than in subsection E, 13.9% and 88.8%, respectively (Table 1). In subsections B and C, internal to the vineyard, diseased vines were randomly distributed. Though subsection D was also internal, increased levels of spatial aggregation were observed, potentially due to its proximity to the disease focus (Fig. 2). These results confirmed that disease spread is dependent on the initial GRBV incidence and eventually on the abundance and behavior of *S. festinus*[14,24,32].

Epidemic dynamics at various spatial scales (2 × 2, 3 × 3, and 4 × 4 quadrats) suggested GRBV spread was mostly from diseased vines to neighboring vines. This may suggest vine-to-vine dispersal of viruliferous *S. festinus* that are traveling or jumping through the vine canopy. Such movement has not been described for *S. festinus* in the vineyard; only longer distance flights have been characterized in the laboratory[37] and inferred in vineyard ecosystems[31]. Nonetheless, walking and jumping alongside flying have been recently identified as movement patterns of *S. festinus* in the laboratory[38]. It would be interesting to validate these dispersal behaviors of *S. festinus* in the vineyard. Additionally, the distribution of GRBV strains within the vineyard provided insight into the nature of spread. Previous work found the disease focus to exclusively consist of GRBV strain 2 with identical genomic sequences, likely due to the use of infected rootstock material[23]. Similar to previously reported findings[14,28,35], no vines tested in this study contained mixed infections of GRBV strains. Further work is needed to assess the potential for coinfection of the two strains, as is observed in other grapevine viruses[39–42], or the occurrence of competitive exclusion. *S. festinus* can transmit both GRBV strains in the laboratory and vineyard[25,28,36] and no significant difference in GRBV titer was found in infected vines for the two strains in June, when *S. festinus* are actively transmitting GRBV from asymptomatic vines, or in October, when disease symptoms peak[35]. Together, there should be ample opportunities for vines to become infected with both strains via *S.* festinus-mediated transmission. More work is needed to address the possibility of competitive exclusion between the two GRBV strains.

The surrounding diseased vines in subsection E were predominantly infected with GRBV strain 2 compared to strain 1 (80.4% and 9.2%, respectively; Table 1). We hypothesize that *S. festinus* entered the vineyard from the neighboring riparian areas or natural vegetation habitats, acquired GRBV from the disease focus, and then spread strain 2 to nearby vines when dispersing, i.e., local dispersal. Conversely, in subsection A and eventually throughout the entire vineyard, *S. festinus* specimens may have carried GRBV strain 1 from infected material outside of the study vineyard, i.e., background sources, such as the nearby GRBV-infected 'Merlot' and 'Cabernet Sauvignon' plantings in which strain 1 is prevalent[14]. However, the introduction of strain 2 from background sources, including infected vineyards or proximal infected free-living vines[14,16], by dispersing *S. festinus* cannot be excluded. A higher incidence of strain 1 than strain 2 was identified on the western side of the vineyard (Fig. 2A). This suggested that vines infected with strain 1 in the western area of the vineyard may have served as a source of inoculum for secondary spread upon introduction, potentially from outside sources.

In red-berried cultivars, red blotch disease incidence is typically determined by visually assessing foliar red blotch symptoms[14,23,34,43]. Our study clearly indicated that virus incidence can be grossly underestimated due to asymptomatic infections (Fig. 2A). Asymptomatic and symptomatic GRBV-infected vines have been previously described in diseased vineyards[25,34,44] but not to the magnitude documented in this study. In subsection C of the study vineyard, 13.8% of vines were infected with GRBV without exhibiting disease symptoms. This incidence is similar to symptomatic vines in this subsection, 15.5% (Table 1). A high percentage of asymptomatic, infected vines (9%, 162/1,783), as documented in the five subsections of the study vineyard in 2023 (Table 1), is unique to GRBV compared with other viruses of grapevine. It may be explained by an unusually long latency period for disease symptoms to become apparent following GRBV inoculation upon *S. festinus*-mediated transmission, as previously suggested[25]. More work is needed to address this important period of disease dynamics and the implications for disease management.

Increases in disease incidence and rate of spread were observed three years following years with less rainfall (Fig. 4). This finding may be explained by the observation that *S. festinus* is more likely to visit vineyards in years with lower precipitation[31] because their feeding and reproductive hosts in natural habitats are unlikely to survive in non-irrigated areas compared to irrigated vineyards. In addition, *S. festinus* is capable of flying over 500 meters[37], making dispersal to feeding hosts, even non-preferred feeding host such as grapevine, during low rainfall years even more likely. A three-year lag from *S. festinus* visiting vineyards to the observation of disease symptoms in addition to the prevalence of asymptomatic infections supports the extended incubation and latency periods observed in GRBV-inoculated grapevines[25,28].

The epidemiological trajectories observed in this study are unique to red blotch disease. No other grapevine viral disease shows similar spread patterns. For example, grapevine leafroll disease epidemics usually start with randomly distributed diseased vines followed by aggregation along rows due to resident mealybug vectors dispersing along the trellis and the vine canopy[45–47]. The logistic model best fits leafroll epidemics[45,47], while both the logistic and exponential models fit red blotch epidemics dependent upon disease incidence (this study). The distinct epidemiological features of red blotch disease are shaped, like leafroll disease, by virus incidence and spatiotemporal aggregation, but also by vector dispersal and weather patterns, unlike in leafroll disease. The fact that a treehopper transmits GRBV while using grapevines as an opportunistic host adds stochasticity and complexity to red-blotch disease dynamics. Furthermore, the fact that wine grapes are not a preferred feeding or reproductive host of *S. festinus* and the feeding damage that results in petiole and shoot girdling does not result in economic losses[29] further complicates our understanding of the GRBV-*S. festinus*-grapevine pathosystem. This begs for behavioral studies of *S. festinus* to better understand the short- and long-distance spread of GRBV documented in this study.

Roguing, the elimination of diseased vines and their replacement with grafted vines derived from GRBV-free scion and rootstock materials, is recommended in red blotch diseased vineyards to reduce virus inoculum and limit secondary virus spread[4,22], particularly in vineyards with confirmed disease spread and *S. festinus* present. A bioeconomic study recommended roguing individual diseased vines if disease incidence was less than 30% and removal of the entire vineyard if disease incidence was greater than 30%[22]. Based on our findings, zonal roguing, the selective removal of diseased vines and surrounding vines (regardless of infection status), is an appropriate response to reduce virus inoculum and limit secondary spread. Zonal roguing aligns well with the previous bioeconomic study[22]. For example, when incidence is less than 20%, and no aggregation is observed, as in subsections B (11.3%), C (15.7%), and E (9.2%, GRBV strain 1), roguing infected vines and six surrounding vines, one neighboring vine on each side within and across rows, and one vine diagonal, could substantially reduce secondary spread (Figs. 3 and 5). When incidence is less than 20% and disease foci are aggregated, as in subsection A (13.9%), roguing two vines on each side of the infected vine within the row, and one vine on each side across the row is recommended (Figs. 3 and 5). When incidence is between 21% and 50%, as in subsection D, our findings suggest roguing three vines on either side within the same row, across rows, and diagonal is appropriate (Figs. 3 and 5). When incidence is between 51% and 85%, as for vines infected with strain 2 in subsection E (80.3%), removing six vines on each side within rows, across rows, and diagonal is recommended (Figs. 3 and 5). Nonetheless, in practice, the latter two scenarios are not recommended as disease incidence should remain below a 30% threshold established by a bioeconomic study[22].

Zonal roguing of seven to 49 vines, as suggested in this study (Fig. 5), is an aggressive response to manage a viral disease in vineyards. Roguing individual vines is commonly practised for the management of grapevine leafroll-associated virus 3, the major viral agent of leafroll disease[46,48–51]. Roguing of the diseased vine and two immediate within-row neighbors on

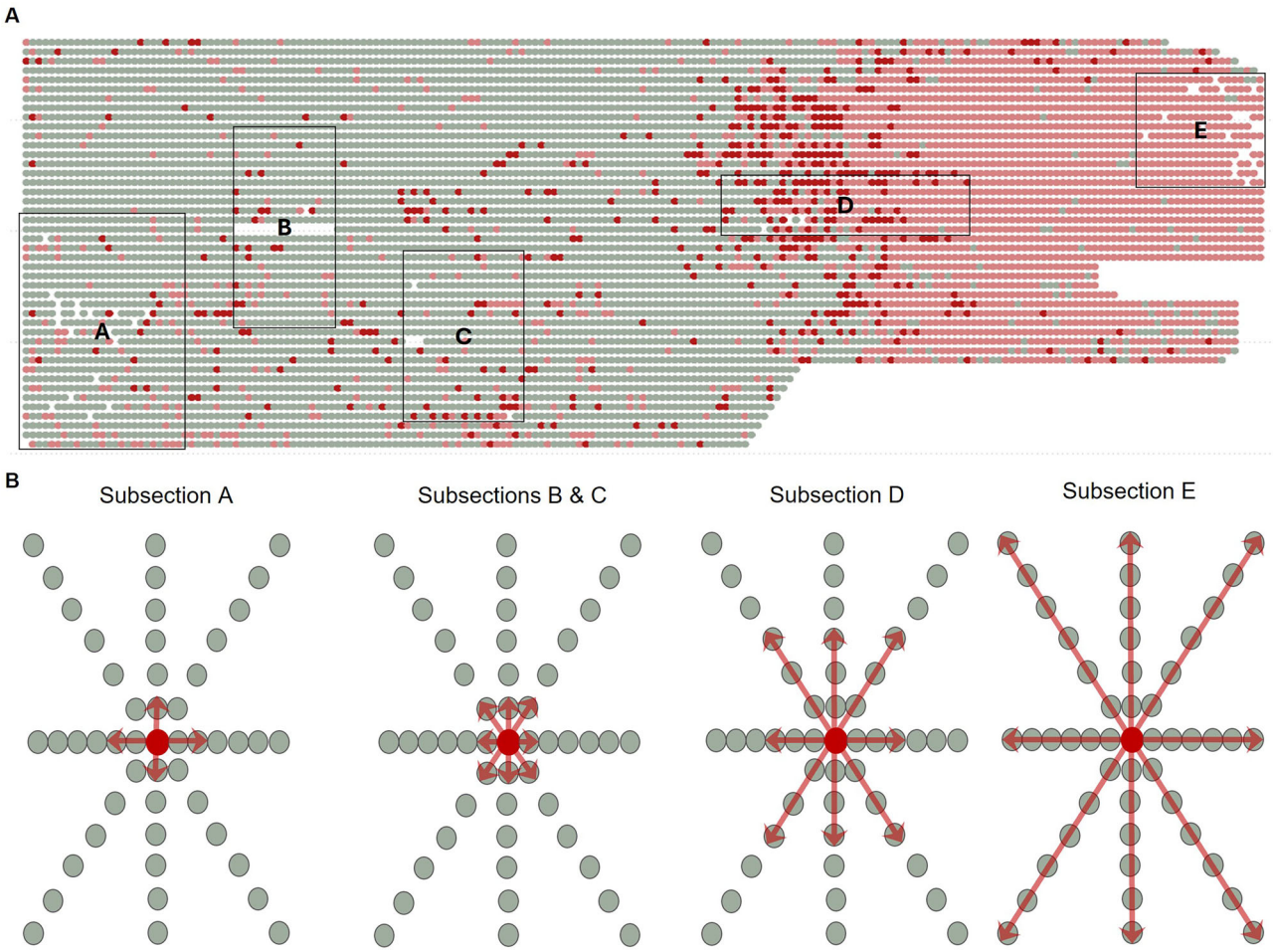

Fig. 5 | Proposed zonal roguing in a red blotch diseased 'Cabernet franc' vineyard in Napa Valley, California. A Red blotch disease incidence map in 2023 with five overlayed subsections in which every vine was assessed visually for symptoms and tested for grapevine red blotch (GRBV) by PCR and used for join-count analysis. **B** Proposed zonal roguing based on disease incidence and aggregation. When incidence is less than 20%, and vines are aggregated as in subsection A, roguing the diseased vine (shown in red) and six surrounding vines is recommended, two on each side within a row and one from each side across the row. When disease incidence is less than 20% and not aggregated, as observed in subsections B and C, roguing of eight vines in addition to the diseased vine is recommended: one vine on each side of the diseased vine within row, across row, and diagonal. When incidence is between 21 and 50% and aggregated, roguing the diseased vine and 24 surrounding vines is recommended: three vines on each side of the diseased vine within a row, across a row and diagonal. When incidence is >51%, roguing the diseased vine and 48 surrounding vines is recommended: six vines on each side of the diseased vine within a row, across a row, and diagonal. Despite these data being statistically supported, maintaining vineyards with incidence >30% is not recommended, based on data shown previously by bioeconomic studies[22].

each side was shown to substantially reduce the spread of grapevine leafroll-associated virus 1[50]. Nonetheless, zonal roguing would be a novel response to a viral pathogen in vineyards. As such, it warrants further attention in future bioeconomic studies to ascertain its economic feasibility. However, zonal roguing should be considered in any vineyard where the secondary spread of GRBV is occurring. This novel roguing strategy also has the potential to combat devastating pathogen infections in other specialty crops, such as citrus greening in citrus groves and banana bunchy top virus in banana plantations.

This is the first study of its kind to monitor viral disease spread in a perennial fruit crop for a decade, contiguously, in relation to weather conditions and to characterize epidemiological attributes of a speciality crop disease caused by a treehopper-transmitted virus. Spread dynamics were shaped by virus incidence, aggregation patterns, vector dispersal and weather. The use of descriptive and quantitative epidemiological statistics provided insights into unique red blotch disease spread trajectories. The intensity of epidemics varied with proximity to an initial disease focus. We documented extensive within-vineyard secondary spread along with the influx of GRBV, likely via *S. festinus*, from background sources, such as adjacent or distant vineyards or proximal free-living vines. This information was paramount to refining red blotch disease management guidelines and proposing zonal roguing as a novel response to a viral disease in a perennial crop.

Methods

Vineyard selection and mapping

A 2-ha 'Cabernet franc' vineyard consisting of clones 214 and 623 grafted onto the rootstock 101–14 Mgt, and established in 2008 in Napa County, California was selected for this study. The vineyard was comprised of 44 rows ranging from 114–195 vines per row with a 1.2 and 2.1 m spacing within and between rows, respectively. The vineyard utilized a vertical shoot positioning system and conventional drip irrigation and pest management practices for vineyards in Napa County throughout the duration of this study.

The incidence of red blotch disease symptoms was mapped during annual surveys in early to mid-October from 2014 to 2023. Data from the 2014 to 2018 assessments were previously published[23,24] and supplemented with disease incidence data from 2019 to 2023 (this study). The presence of the insect vector of GRBV, *S. festinus*, was reported in the vineyard in 2015 and 2016[32].

Vineyard subsection selection and tissue collection

Within the 'Cabernet franc' vineyard, five rectangular subsections (A-E) were chosen for high-resolution assessments of disease incidence and spread (Fig. 2A). These subsections ranged from 240 to 625 vines. Disease incidence was greater than 5% in these five subsections in 2021 based on visual symptoms. These subsections were selected to represent vineyard areas with varying disease incidence and levels of aggregation. Some subsections were along the vineyard edges with low disease incidence (subsections A and C), while others were central areas of the vineyard with variable disease incidence and proximity to an existing disease focus (subsections B and D). Subsection E was encompassed entirely in the primary disease foci. In October 2022 and 2023, six leaves and petioles were collected from the base of the canopy of every vine, with or without red blotch disease symptoms, spanning both cordons from within each of the five subsections. In total, tissue was collected from 1783 vines for GRBV detection by PCR. Petioles were processed for GRBV testing, as previously described[14,28].

Detection of GRBV and isolate characterization

Nucleic acids were isolated from grapevine petioles using the MagMAX-96 Al/ND Isolation Kit (ThermoFisher Scientific, Waltham, MA) on a King-Fisher instrument (ThermoFisher Scientific, Waltham, MA). The presence of GRBV was determined via multiplex PCR using primer pairs amplifying fragments of the open reading frames coding the coat protein and RepA replication-associated protein[4,5,14,28]. Amplicons were analyzed by electrophoresis on agarose gels and visualized by UV illumination after staining with GelRed (Biotium, Fremont, CA).

GRBV isolates in infected leaf samples were further characterized by restriction fragment length polymorphism to identify strains 1 and 2, as previously described[28]. Briefly, amplicons using the above-described primer pair corresponding to the GRBV RepA genomic region underwent restriction digestion using AleI-v2 (New England Biolabs, Ipswich, MA) to distinguish strains 1 and 2[28]. Digestions were resolved by electrophoresis on agarose gels as described above. Significant differences in the incidence of vines infected with GRBV for each year within each subsection were determined via pairwise t test with $\alpha = 0.05$. Analyses were conducted for strain 1 and strain 2 infected vines for each year and subsection.

Temporal analyses

Monomolecular, exponential, logistic, and Gompertz models were fitted to red blotch disease incidence over time by non-linear regression with the *nlsLM* function of the *MINPACK.LM* package[52]. The model of best fit was selected based on the larger coefficient of determination (R^2), lower root mean square error, independence and homogeneity of variances, in addition to the lower second-order Akaike's Information Criterion corrected for smaller sample sizes, and larger maximum likelihood fit[53–56]. The best model for each data set was used to estimate disease incidence at epidemic initiation (y_0), disease rate (r), incidence at the last assessment (y_{max}), and expected duration to reach a disease incidence of 50% (y_{50})[57]. Significant differences in disease incidence and GRBV strain incidence were determined using pairwise t tests ($\alpha = 0.05$). Analyses were conducted on the entire study vineyard and all five individual subsections for each GRBV strain.

Spatiotemporal analyses

The index of dispersion (D) was calculated as the ratio of the observed variance and estimated, theoretical binomial variance[58]. When $D = 1$, the pattern of diseased vines is interpreted as random, with aggregation indicated when $D > 1$. The degree of aggregation is directly proportional to the magnitude of D. A χ^2 statistic was performed to test if $D = 1$[59]. Analyses were performed at different spatial scales of the entire vineyard and individual subsections using the *EPIPHY* package[60] in the software R[61].

The binomial and beta-binomial distributions were fitted to the disease incidence datasets of the full vineyard, and each individual subsection provided a complimentary statistical check on the spatial pattern of symptomatic vines[59,62,63]. The binomial model represents the probability of a vine being diseased, with a single parameter, π, across all sampling units, and assumes a random distribution. If the binomial assumption is violated, the beta-binomial distribution was used to detect if diseased vines are over-dispersed (i.e., aggregated or clustered). The beta-binomial distribution model accounts for additional heterogeneity by incorporating an additional parameter, θ, a measure of variation in disease probability among sampling units[59,62,63]. Each parameter was estimated by maximum likelihood[64] and fit distributions determined by the χ^2 goodness-of-fit test. When the binomial assumption of randomness was not rejected ($\theta = 0$), the pattern of diseased vines was interpreted as random. When the binomial assumption was violated, the beta-binomial model indicated diseased vines were aggregated ($\theta > 0$). A log-likelihood ratio test was also performed to identify when the beta-binomial distribution provided a better fit to the incidence data than the binomial distribution[59,62]. These analyses were performed within the *EPIPHY* package[60] in the R software[61].

Geostatistical-based analyses

Data on GRBV infection in each of the five subsections of the vineyard was also analyzed using join-count statistics[65,66] to determine if neighboring vines (within rows, across rows, or diagonally across rows) at varying spatial distances (lags) were more likely to have the same (or opposite) status of GRBV infection, or different strains, i.e., 1 or 2, compared to being distributed randomly. The analysis was conducted in each subsection encompassing the two GRBV strains considered together and individually in 2023, the final observation year. For each data set, join-count statistics were used to calculate the observed and expected number of join-counts and standard deviation or the expected value under the null hypothesis of a random pattern varying from one to six lags. A Z statistic was used to determine whether the observed number of joins was significantly ($Z \leq -1.96$) different from the expected number of joins under the null hypothesis of randomness. The incidence of diseased vines in subsections D and E was too high (>70%) to conduct join-count analyses and hence excluded. This analysis was conducted with the SAS Statistical Software (Cary, NC, USA).

Disease patterns were also analyzed using the Spatial Analysis by Distance IndicEs (SADIE)[67–71] at the scale of the entire vineyard, SADIE was performed on quadrats of 2×2, 3×3, and 4×4 vines. Individual vineyard subsections were analyzed by SADIE using 2×2 quadrats. This test uses a distance-to-regularity algorithm (D_r)[69] to calculate an index of aggregation (I_a), the ratio of the observed distance to regularity by the expected value for a random spatial pattern. When $I_a = 1$, a random spatial pattern is suggested, whereas $I_a > 1$ indicates an aggregated pattern. A two-sided hypothesis (H_0: $I_a = 1$) was used to test for deviation of I_a from the null hypothesis of randomness[71]. The analysis was performed with the *EPIPHY* package[60] within the R[61], with a correction for local clustering[67] and 499 randomizations for each data set over the 10-year monitoring study.

Weather data

Weather data were collected from the California Irrigation Management Information System[72]. The weather station, Oakville #77, in Napa County, California, ~2.5 km from the vineyard site, was used for data collection. Maximum and minimum air temperatures (°C) and precipitation (mm) were retrieved. Readings were averaged to obtain monthly and seasonal values from 2010 through 2023 and used in subsequent statistical analyses.

Associations between weather data and GRBV epidemic variables

The associations between y and dy/dt and weather variables (maximum and minimum air temperatures and precipitation) were calculated using a Pearson's correlation coefficient and visualized using a heat map correlogram with the *Hmisc* package[73] in R software. The correlogram was created using Pearson correlation coefficients to evaluate associations among the main epidemic variables obtained over 10 years and local weather data in two seasons, spring (March–June) and summer (June–September). The correlation coefficients were calculated for the relationships up to four seasonal lags (years) from the year of interest for y and dy/dt, due to the extended latency period of GRBV[25].

Data availability

Extended data files including disease incidence and statistical information is available in supplementary material. Additional raw data will be made available upon request.

Code availability

The statistical packages used in this study were previously published but tailored codes will be made available upon request.

Received: 23 November 2024; Accepted: 31 March 2025;
Published online: 15 April 2025

References

1. Jeger, M. J. The epidemiology of plant virus disease: towards a new synthesis. *Plants* **9**, 1768 (2020).
2. Jones, R. A. C. Plant virus ecology and epidemiology: historical perspectives, recent progress and future prospects. *Ann. Appl. Biol.* **164**, 320–347 (2014).
3. Calvi, B. L. Effects of red-leaf disease on cabernet sauvignon at the Oakville experimental vineyard and mitigation by harvest delay and crop adjustment. http://www.semanticscholar.org/paper/Effects-Of-Red-leaf-Disease-On-Cabernet-Sauvignon-Calvi/56c03172529e5696f93699ae137baefd0065b9eb (2011).
4. Cieniewicz, E., Perry, K. & Fuchs, M. Grapevine red blotch: molecular biology of the virus and management of the disease. In: *Grapevine Viruses: Molecular Biology, Diagnostics and Management* (eds. Meng, B., Martelli, G. P., Golino, D. A. & Fuchs, M.) 303–314 https://doi.org/10.1007/978-3-319-57706-7_14. (Springer International Publishing, Cham, 2017).
5. Krenz, B., Thompson, J. R., McLane, H. L., Fuchs, M. & Perry, K. L. Grapevine red blotch-associated virus is widespread in the United States. *Phytopathology* **104**, 1232–1240 (2014).
6. Rumbaugh, A. C. et al. Impact of rootstock and season on red blotch disease expression in cabernet sauvignon (*V. vinifera*). *Plants* **10**, 1583 (2021).
7. Sudarshana, M. R., Perry, K. L. & Fuchs, M. F. Grapevine red blotch-associated virus, an emerging threat to the grapevine industry. *Phytopathology* **105**, 1026–1032 (2015).
8. National Academy of Sciences, Engineering, and Medicine. Advancing vineyard health: insights and innovations for combating grapevine red blotch and leafroll diseases. (eds. The National Academies Press) https://doi.org/10.17226/27472 (2024).
9. Yepes, L. M. et al. Causative role of grapevine red blotch virus in red blotch disease. *Phytopathology* **108**, 902–909 (2018).
10. Al Rwahnih, M., Rowhani, A. & Golino, D. First report of grapevine red blotch-associated virus in archival grapevine material from Sonoma County, California. *Plant Dis.* **99**, 895–895 (2015).
11. Ouro-Djobo, A. et al. Molecular characterization of divergent isolates of grapevine red blotch virus from Blanc du Soleil, an interspecific hybrid white grapevine cultivar. *PhytoFront* **3**, 290–295 (2023).
12. Schoelz, J. et al. A survey of viruses found in grapevine cultivars grown in Missouri. *Am. J. Enol. Vitic.* **72**, 73–84 (2021).
13. Soltani, N. et al. A survey for nine major viruses of grapevines in Tennessee vineyards. *Plant Health Prog.* **21**, 157–161 (2020).
14. Flasco, M. T., Cieniewicz, E. J., Pethybridge, S. J. & Fuchs, M. F. Distinct red blotch disease epidemiological dynamics in two nearby vineyards. *Viruses* **15**, 1184 (2023).
15. Bahder, B. W., Zalom, F. G. & Sudarshana, M. R. An evaluation of the flora adjacent to wine grape vineyards for the presence of alternative host plants of grapevine red blotch-associated virus. *Plant Dis.* **100**, 1571–1574 (2016).
16. Perry, K. L. et al. Grapevine red blotch-associated virus is present in free-living *Vitis* spp. proximal to cultivated grapevines. *Phytopathology* **106**, 663–670 (2016).
17. Cieniewicz, E. et al. Prevalence and genetic diversity of grabloviruses in free-living *Vitis* spp. *Plant Dis.* **102**, 2308–2316 (2018).
18. KC, A. N., DeShields, J. B., Levin, A. D., Hilton, R. & Rijal, J. Epidemiology of grapevine red blotch disease progression in southern Oregon vineyards. *Am. J. Enol. Vitic.* **73**, 116–124 (2022).
19. Al Rwahnih, M. et al. Association of a DNA virus with grapevines affected by red blotch disease in California. *Phytopathology* **103**, 1069–1076 (2013).
20. Blanco-Ulate, B. et al. Red blotch disease alters grape berry development and metabolism by interfering with the transcriptional and hormonal regulation of ripening. *J. Exp. Bot.* **68**, 1225–1238 (2017).
21. Cauduro Girardello, R. et al. The impact of grapevine red blotch disease on *Vitis vinifera* L. Chardonnay grape and wine composition and sensory attributes over three seasons. *J. Sci. Food Agric.* **100**, 1436–1447 (2020).
22. Ricketts, K. D. et al. Mitigating the economic impact of grapevine red blotch: optimizing disease management strategies in U.S. vineyards. *Am. J. Enol. Vitic.* **68**, 127–135 (2017).
23. Cieniewicz, E. J. et al. Spatiotemporal spread of grapevine red blotch-associated virus in a California vineyard. *Virus Res.* **241**, 156–162 (2017).
24. Cieniewicz, E. et al. Differential spread of grapevine red blotch virus in California and New York vineyards. *Phytobiomes J.* **3**, 203–211 (2019).
25. Flasco, M., Cieniewicz, E. J., Cooper, M. L., McLane, H. & Fuchs, M. Investigating the latency period of grapevine red blotch virus in a diseased Cabernet franc vineyard experiencing secondary spread. *Am. J. Enol. Vitic*. **75**, 0750018 (2024).
26. Dalton, D. T. et al. Spatial associations of vines infected with grapevine red blotch virus in Oregon vineyards. *Plant Dis.* **103**, 1507–1514 (2019).
27. Flasco, M. et al. Grapevine red blotch virus is transmitted by the three-cornered alfalfa hopper in a circulative, nonpropagative mode with unique attributes. *Phytopathology* **111**, 1851–1861 (2021).
28. Flasco, M. T. et al. The three-cornered alfalfa hopper, *Spissistilus festinus*, is a vector of grapevine red blotch virus in vineyards. *Viruses* **15**, 927 (2023).
29. Preto, C. R., Bahder, B. W., Bick, E. N., Sudarshana, M. R. & Zalom, F. G. Seasonal dynamics of *Spissistilus festinus* (Hemiptera: Membracidae) in a Californian vineyard. *J. Econ. Entomol.* **112**, 1138–1144 (2019).
30. Wilson, H., Yazdani, A. S. & Daane, K. M. Influence of riparian habitat and ground covers on threecornered alfalfa hopper (Hemiptera: Membracidae) populations in vineyards. *J. Econ. Entomol.* **113**, 2354–2361 (2020).
31. Hoyle, V. et al. Connectivity of plant communities for viral disease dynamics informed by the dietary profiles of a treehopper. *Phytobiomes J*. https://doi.org/10.1094/PBIOMES-11-24-0105-R (2025).
32. Cieniewicz, E. J., Pethybridge, S. J., Loeb, G., Perry, K. & Fuchs, M. Insights into the ecology of grapevine red blotch virus in a diseased vineyard. *Phytopathology* **108**, 94–102 (2018).
33. Setiono, F. J., Chatterjee, D., Fuchs, M., Perry, K. L. & Thompson, J. R. The distribution and detection of grapevine red blotch virus in its host depend on time of sampling and tissue type. *Plant Dis.* **102**, 2187–2193 (2018).
34. DeShields, J. B. & KC, A. N. Comparative diagnosis of grapevine red blotch disease by endpoint PCR, qPCR, LAMP, and visual symptoms. *Am. J. Enol. Vitic*. **74**, 0740015 (2023).
35. Flasco, M. et al. Seasonal variation in grapevine red blotch virus titer in relation to disease symptom expression in vineyards. *Phytobiomes J.* **8**, 192–200 (2024).
36. Hoyle, V. et al. Transmission of grapevine red blotch virus by *Spissistilus festinus* [Say, 1830] (Hemiptera: Membracidae) between free-living vines and *Vitis vinifera* 'Cabernet Franc. *Viruses* **14**, 1156 (2022).
37. Antolínez, C. A., Chandler, M., Hoyle, V., Fuchs, M. & Rivera, M. J. Differential flight capacity of *Spissistilus festinus* (Hemiptera: Membracidae) by sex and age. *J. Insect Behav.* **36**, 347–357 (2023).

38. Hoyle, V. J., Schultz, M., McGinnity Schneider, E. J., Roy, B. G. & Fuchs, M. Lack of vertical transmission of grapevine red blotch virus by *Spissistilus festinus* and sex-associated differences in horizontal transmission. *Insects* **15**, 1014 (2024).
39. Fiore, N. et al. Survey of grapevine viruses in Chile. *J. Plant Pathol.* **90**, 125–130 (2008).
40. Sharma, A. M. et al. Relative prevalence of grapevine leafroll-associated virus species in wine grape-growing regions of California. *PLoS One* **10**, e0142120 (2015).
41. Vigne, E., Garcia, S., Komar, V., Lemaire, O. & Hily, J.-M. Comparison of serological and molecular methods with high-throughput sequencing for the detection and quantification of grapevine fanleaf virus in vineyard samples. *Front. Microbiol*. **9**, 2726 (2018).
42. Kubina, J. et al. Characterization of grapevine fanleaf virus isolates in 'chardonnay' vines exhibiting severe and mild symptoms in two vineyards. *Viruses* **14**, 2303 (2022).
43. Rohrs, J. K., Fendell-Hummel, H. G., MacDonald, S. L. & Cooper, M. L. Best practices for monitoring visual symptoms of grapevine red blotch disease in black-fruited winegrape cultivars. *Am. J. Enol. Vitic.* **74**, 0740036 (2023).
44. Rohrs, J. K., Fendell-Hummel, H. G., MacDonald, S. L., Hobbs, M. B. & Cooper, M. L. Trunk cambium facilitates pre-symptomatic and year-round detection of grapevine red blotch virus using the LAMP assay. *Am. J. Enol. Vitic*. **75**, 0750023 (2024).
45. Arnold, K., Golino, D. A. & McRoberts, N. A synoptic analysis of the temporal and spatial aspects of grapevine leafroll disease in a historic Napa vineyard and experimental vine blocks. *Phytopathology* **107**, 418–426 (2017).
46. Cabaleiro, C. & Segura, A. Temporal analysis of grapevine leafroll associated virus 3 epidemics. *Eur. J. Plant Pathol.* **114**, 441–446 (2006).
47. Donda, B. P., Kesoju, S. R., Arnold, K., McRoberts, N. & Naidu, R. A. Spatio-temporal spread of grapevine leafroll disease in Washington state vineyards. *Plant Dis.* **107**, 1471–1480 (2023).
48. Pietersen, G. et al. Control of grapevine leafroll disease spread at a commercial wine estate in South Africa: a Case Study. *Am. J. Enol. Vitic.* **64**, 296–305 (2013).
49. Bell, V. A., Hedderley, D. I., Pietersen, G. & Lester, P. J. Vineyard-wide control of grapevine leafroll-associated virus 3 requires an integrated response. *J. Plant Pathol.* **100**, 399–408 (2018).
50. Hesler, S. et al. Spatial roguing reduces the incidence of leafroll disease and curtails its spread in a Finger Lakes Cabernet franc vineyard. *Am. J. Enol. Vitic.* **73**, 227–236 (2022).
51. Hobbs, M. B. et al. Adoption of best management practices for grapevine leafroll and red blotch diseases: a survey of West Coast growers. *PhytoFront* **2**, 181–191 (2022).
52. Elzhov, T. V., Mullen, K. M., Spiess, A.-N. & Bolker, B. CRAN - package minpack.lm. (2016).
53. Akaike, H. Information theory and an extension of the maximum likelihood principle. In: *Selected Papers of Hirotugu Akaike* (eds. Parzen, E., Tanabe, K. & Kitagawa, G.) 199–213 https://doi.org/10.1007/978-1-4612-1694-0_15. (Springer, New York, NY, 1998).
54. Sugiura, N. Further analysis of the data by Akaike's information criterion and the finite corrections: Further analysis of the data by akaike' s. *Commun. Stat. Theory Methods* **7**, 13–26 (1978).
55. Hurvich, C. M. & Tsai, C.-L. Bias of the corrected |mathromAIC criterion for underfitted regression and time series models. *Biometrika* **78**, 499–509 (1991).
56. Hurvich, C. M. & Tsai, C. W. Regression and time series model selection in small samples. *Biometrika* **76**, 297–307 (1989).
57. Simko, I. & Piepho, H.-P. The area under the disease progress stairs: calculation, advantage, and application. *Phytopathology* **102**, 381–389 (2012).
58. Madden, L. V., Hughes, G. & van den Bosch, F. The study of plant disease epidemics. (ed. American Phytopathological Society Press, St. Paull, MN, 2017).
59. Madden, L. V. & Hughes, G. Plant disease incidence: distributions, heterogeneity, and temporal analysis. *Annu. Rev. Phytopathol.* **33**, 529–564 (1995).
60. Gigot, C. _epiphy: analysis of plant disease epidemics_. (2023).
61. R Core Team. R: a language and environment for statistical computing. (2023).
62. Madden, L. V., Hughes, G., Moraes, W. B., Xu, X.-M. & Turechek, W. W. Twenty-five years of the binary power law for characterizing heterogeneity of disease incidence. *Phytopathology* **108**, 656–680 (2018).
63. Turechek, W. W., Madden, L. V., Gent, D. H. & Xu, X.-M. Comments regarding the binary power law for heterogeneity of disease incidence. *Phytopathology* **101**, 1396–1407 (2011).
64. Smith, D. M. Algorithm AS 189: maximum likelihood estimation of the parameters of the beta binomial distribution. *J. R. Stat. Soc. Ser. C. Appl. Stat.* **32**, 196–204 (1983).
65. Moran, P. A. P. The interpretation of statistical maps. *J. R. Stat. Soc. Ser. B. Methodol.* **10**, 243–251 (1948).
66. Upton, G. & Fingleton, B. Spatial data analysis by example. Vol. 1: point pattern and quantitative data. (ed. John Wiley & Sons, Chichester) (1985).
67. Li, B., Madden, L. V. & Xu, X. Spatial analysis by distance indices: an alternative local clustering index for studying spatial patterns. *Methods Ecol. Evol.* **3**, 368–377 (2012).
68. Perry, J. N. Spatial analysis by distance indices. *J. Anim. Ecol.* **64**, 303–314 (1995).
69. Perry, J. N. Measures of spatial pattern for counts. *Ecology* **79**, 1008–1017 (1998).
70. Perry, J. N., Winder, L., Holland, J. M. & Alston, R. D. Red–blue plots for detecting clusters in count data. *Ecol. Lett.* **2**, 106–113 (1999).
71. Xu, X. & Madden, L. V. Interrelationships among SADIE indices for characterizing spatial patterns of organisms. *Phytopathology* **95**, 874–883 (2005).
72. California Department of Water Resources. California irrigation management information system. https://cimis.water.ca.gov/Default.aspx (2024).
73. Harrell, F. Hmisc: a package of miscellaneous R functions. (2014).

Acknowledgements

We are grateful to St. Supery Vineyard and Estates for providing access to their vineyard over the course of this study. We thank Morgan Brett and Josh Anstey for their initial disease observation and mapping. We greatly appreciate the assistance in tissue processing and testing by Fu-Wah Choi, Kyle Hegel, and Rosemary Cox. This work is supported by the California Department of Agriculture (17-0517-000-SA, 19-0262-000-SA, 20-0264-000-SA, 21-0267-000-SA, 22-0552-000-SA) and Cornell Venture Funds.

Author contributions

Conceptualization, methodology, and validation: M.T.F., E.J.C., and M.F.F; formal analysis: M.T.F., E.J.C., D.W.H., and S.J.P.; investigation and data curation: M.T.F., E.J.C., M.L.C, and M.F.F.; writing-original draft preparation: M.T.F. and M.F.F.; writing-reviewing and editing: M.T.F., D.W.H, E.J.C., M.L.C., S.J.P., and M.F.F.; project administration and funding acquisition: M.F.F. All authors have read and agreed to the published version of this manuscript.

Competing interests

The authors declare no competing interests.

Additional information

Supplementary information The online version contains supplementary material available at https://doi.org/10.1038/s44298-025-00111-2.

Correspondence and requests for materials should be addressed to M. T. Flasco.